RESEARCH ARTICLE

Single and Dual Targeting of Mutant EGFR with an Allosteric Inhibitor

Ciric To[1,2,3], Jaebong Jang[4,5], Ting Chen[1], Eunyoung Park[4,5], Mierzhati Mushajiang[1], Dries J.H. De Clercq[4,5], Man Xu[6], Stephen Wang[6], Michael D. Cameron[7], David E. Heppner[4,5], Bo Hee Shin[1,2,3], Thomas W. Gero[4,5], Annan Yang[2], Suzanne E. Dahlberg[8], Kwok-Kin Wong[1,2,3,6], Michael J. Eck[4,5], Nathanael S. Gray[4,5], and Pasi A. Jänne[1,2,3,6]

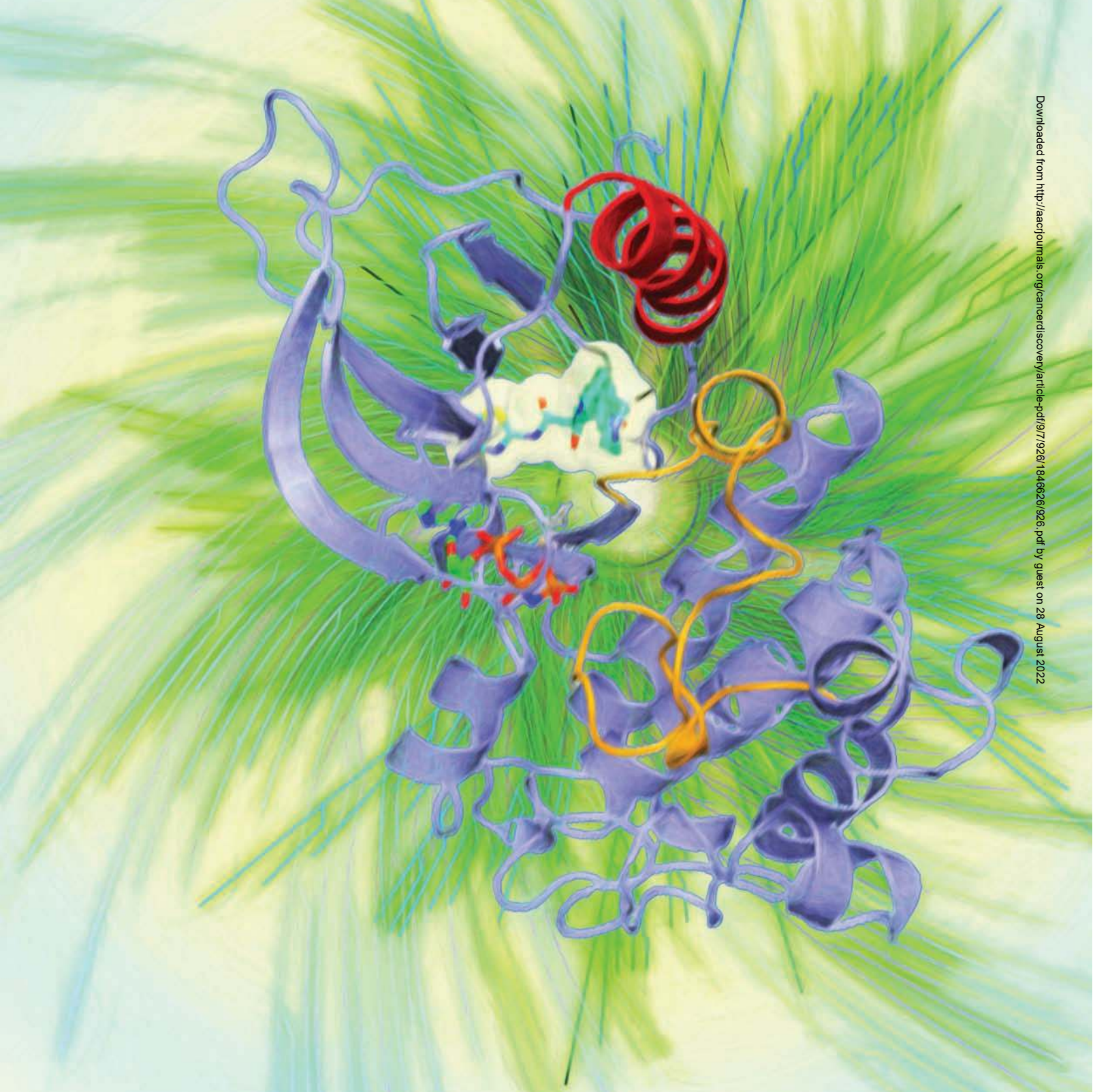

ABSTRACT Allosteric kinase inhibitors offer a potentially complementary therapeutic strategy to ATP-competitive kinase inhibitors due to their distinct sites of target binding. In this study, we identify and study a mutant-selective EGFR allosteric inhibitor, JBJ-04-125-02, which as a single agent can inhibit cell proliferation and EGFR$^{L858R/T790M/C797S}$ signaling *in vitro* and *in vivo*. However, increased EGFR dimer formation limits treatment efficacy and leads to drug resistance. Remarkably, osimertinib, an ATP-competitive covalent EGFR inhibitor, uniquely and significantly enhances the binding of JBJ-04-125-02 for mutant EGFR. The combination of osimertinib and JBJ-04-125-02 results in an increase in apoptosis, a more effective inhibition of cellular growth, and an increased efficacy *in vitro* and *in vivo* compared with either single agent alone. Collectively, our findings suggest that the combination of a covalent mutant–selective ATP-competitive inhibitor and an allosteric EGFR inhibitor may be an effective therapeutic approach for patients with *EGFR*-mutant lung cancer.

SIGNIFICANCE: The clinical efficacy of EGFR tyrosine kinase inhibitors (TKI) in *EGFR*-mutant lung cancer is limited by acquired drug resistance, thus highlighting the need for alternative strategies to inhibit EGFR. Here, we identify a mutant EGFR allosteric inhibitor that is effective as a single agent and in combination with the EGFR TKI osimertinib.

INTRODUCTION

The discovery of activating mutations in EGFR, detected in 10% to 30% of patients with non–small cell lung cancer (NSCLC), has revolutionized the treatment of this disease (1–3). Until recently, EGFR tyrosine kinase inhibitors (TKI), including erlotinib, gefitinib, and afatinib, have been the standard-of-care initial therapy for patients with advanced *EGFR*-mutant lung cancer (4–6). However, despite the initial remarkable response, patients inevitably develop acquired drug resistance within 9 to 14 months of treatment. The most common mechanism of drug resistance, detected in 60% of these patients, is the *EGFR*^{T790M} mutation (7). This secondary mutation increases the affinity of ATP for the binding site, thus outcompeting the binding of the reversible EGFR TKIs gefitinib and erlotinib (8).

Mutant-selective EGFR inhibitors, including the tool compound WZ4002 and the FDA-approved osimertinib (AZD9291; AstraZeneca), are significantly more effective against mutant forms of EGFR (both the activating mutants and T790M) compared with wild-type EGFR (9, 10). In patients with *EGFR*^{T790M}-mediated drug resistance, osimertinib treatment leads to a response rate (RR) of 62% to 71% and progression-free survival (PFS) of 9.9 to 12.3 months and is more effective than chemotherapy (11–13). As initial therapy in patients with advanced *EGFR*-mutant NSCLC, the RR and PFS of osimertinib were 77% and 19.3 months, respectively, suggesting a potential role for osimertinib as a first-line EGFR inhibitor (14). In a phase III clinical trial, osimertinib was more effective than gefitinib or erlotinib (PFS 18.9 vs. 10.2 months; ref. 15). Despite its efficacy, *EGFR*^{C797S}, a tertiary mutation detected in 20% to 25% of patients, has emerged as the most common mechanism of on-target osimertinib resistance (16, 17). C797 is the site of covalent binding for all known irreversible EGFR inhibitors and, as these agents are obligate covalent binders, they become 100 to 1,000-fold less effective at inhibiting cell proliferation and EGFR phosphorylation in the presence of the C797S mutation (9, 17). As such, strategies to treat or prevent osimertinib resistance and/or approaches to more effectively inhibit EGFR may ultimately lead to improved clinical therapies for *EGFR*-mutant patients.

We previously identified the mutant-selective allosteric EGFR inhibitor EAI045 (18). As mutations that impart resistance to ATP-competitive EGFR inhibitors are not located in the allosteric site, EAI045 was effective both *in vitro* and *in vivo* in *EGFR*-mutant models including those harboring the C797S mutation (18). However, it was not effective as a single agent, and required the coadministration of the anti-EGFR antibody cetuximab. The requirement for cetuximab derives from the tendency for EGFR mutants to undergo asymmetrical dimerization (19). In the active dimer, the C-lobe of the activator subunit is bound to the N-lobe of the receiver subunit, thereby impeding the binding of the allosteric inhibitor

[1]Lowe Center for Thoracic Oncology, Dana-Farber Cancer Institute, Boston, Massachusetts. [2]Department of Medical Oncology, Dana-Farber Cancer Institute, Boston, Massachusetts. [3]Department of Medicine, Harvard Medical School, Boston, Massachusetts. [4]Department of Cancer Biology, Dana-Farber Cancer Institute, Boston, Massachusetts. [5]Department of Biological Chemistry and Molecular Pharmacology, Harvard Medical School, Boston, Massachusetts. [6]Belfer Center for Applied Cancer Science, Boston, Massachusetts. [7]Department of Molecular Therapeutics, The Scripps Research Institute, Jupiter, Florida. [8]Department of Biostatistics and Computational Biology, Dana-Farber Cancer Institute, Boston, Massachusetts.

Note: Supplementary data for this article are available at Cancer Discovery Online (http://cancerdiscovery.aacrjournals.org/).

C. To and J. Jang contributed equally to this article.

Corresponding Authors: Pasi A. Jänne, Dana-Farber Cancer Institute, 450 Brookline Avenue, LC-4114, Boston, MA 02215. Phone: 617-632-6076; Fax: 617-582-7683; E-mail: pasi_janne@dfci.harvard.edu; Nathanael S. Gray, Dana-Farber Cancer Institute, 450 Brookline Avenue, LC-2209, Boston, MA 02215. Phone: 617-582-8590; E-mail: nathanael_gray@dfci.harvard.edu; and Michael J. Eck, Dana-Farber Cancer Institute, 450 Brookline Avenue, LC-4313, Boston, MA 02215. Phone: 617-632-5860; E-mail: michael_eck@dfci.harvard.edu

Cancer Discov 2019;9:926–43.

doi: 10.1158/2159-8290.CD-18-0903

to its binding site on the receiver subunit. Cetuximab disrupts EGFR dimers, allowing EAI045 to bind all allosteric sites and consequently to effectively inhibit EGFR. However, the clinical translation of this treatment approach is potentially limited as cetuximab is not EGFR mutant–specific, thereby resulting in on-target wild-type EGFR-mediated toxicities.

In this study, we identify a novel allosteric inhibitor, JBJ-04-125-02, which is effective as a single agent in both *in vitro* and *in vivo* models of *EGFR*-mutant (including C797S) lung cancer. We characterize its mechanism of action and evaluate whether it could augment the efficacy of existing ATP-competitive EGFR inhibitors.

RESULTS

Identification of the Mutant-Selective Allosteric Inhibitor JBJ-04-125-02

To identify a more potent allosteric EGFR inhibitor than EAI045, specifically one that may no longer require the coadministration of cetuximab, we used an iterative process of synthesizing structural analogues of EAI001 and evaluating their efficacy in $EGFR^{L858R/T790M}$ Ba/F3 cells and in biochemical assays with the mutant kinase (18). Functionalization of the isoindolinone moiety at carbon 6 was generally well tolerated, and in some cases yielded enhanced potency relative to EAI001. The compound JBJ-02-112-05, which has a 5-indole substituent appended to the isoindolinone moiety (Fig. 1A), exhibited a biochemical potency of 15 nmol/L for $EGFR^{L858R/T790M}$ (Fig. 1B). Further optimization led to JBJ-04-125-02, which incorporates the potency-enhancing 2-hydroxy-5-fluorophenyl group of EAI045 and a phenylpiperazine on the isoindolinone (Fig. 1A). JBJ-04-125-02 exhibited subnanomolar potency against $EGFR^{L858R/T790M}$ in biochemical assays (IC_{50} = 0.26 nmol/L; Fig. 1B).

The crystal structure (Supplementary Table S1) of JBJ-04-125-02–bound T790M-mutant EGFR reveals that the compound binds to the allosteric pocket of EGFR that is generated by the outward displacement of αC-helix in the inactive kinase conformation (Fig. 1C). The binding modes of the thiazoleamide, phenyl ring, and isoindolinone resemble those of EAI001 observed previously (18). In addition, the hydroxyl group makes a hydrogen bond with the carbonyl group of the Phe856 in the DFG motif. The 4-piperazinophenyl substituent extends along the αC-helix to the solvent exposed exterior, and its phenyl ring makes a π-π stacking interaction with Phe723 in the kinase P-loop. Interestingly, binding of the compound induces a novel conformation of the kinase activation loop that appears to be stabilized by a hydrogen bond between the piperazine and Glu865 in the activation loop (Fig. 1C). In addition, Glu749 is positioned toward the hydrogen bond with the piperazine group (Fig. 1C). We expect that the reconfigured activation loop and the resulting hydrogen bonds to the piperazine group contribute to the enhanced potency of this compound as compared with EAI045. However, we note that the hydrogen bonds to the piperazine are present in only 2 of the 6 unique molecules in this crystal form. In the remaining molecules, the activation loop is partially disordered and the side chain of Glu749 extends away from the compound.

Kinome selectivity profiling (at 10 μmol/L) against a panel of 468 kinases using the KINOME*scan* approach (20) revealed that JBJ-04-125-02 has excellent selectivity across the human kinome with S-Score [35] = 0.02 (Fig. 1D; Supplementary Table S2A and S2B). Only three non-ERBB family members were inhibited at the 35% cutoff: MAP4K5 (% control: 9.5), TIE1 (% control: 29), and TIE2 (% control: 33). As expected, JBJ-04-125-02 lacks binding affinity against Del_19-containing EGFR mutants where the inward disposition of the αC-helix results in the closing of the potential allosteric binding pocket (Supplementary Table S2A).

JBJ-04-125-02 Is Effective as a Single Agent in *EGFR*^{C797S} Models *In Vitro* and *In Vivo*

We tested the ability of JBJ-04-125-02 to inhibit cell proliferation in a panel of Ba/F3 cell lines that were stably transfected with $EGFR^{L858R}$, $EGFR^{L858R/T790M}$, or $EGFR^{L858R/T790M/C797S}$ mutations (Fig. 2A; Supplementary Table S2C). JBJ-04-125-02 was the only compound that could inhibit cell proliferation as a single agent (Fig. 2A; Supplementary Fig. S1A). JBJ-04-125-02 did not inhibit the growth of parental Ba/F3 or wild-type EGFR Ba/F3 cells. Notably, JBJ-04-125-02 was also the most potent when compared with EAI045 and JBJ-02-112-05 and when combined with cetuximab (Supplementary Fig. S1A). Consistent with the kinome selectivity profiling, Ba/F3 cells harboring any of the $EGFR^{Del\_19}$ variants were resistant to JBJ-04-125-02 (Supplementary Table S2C). We next examined the ability of EAI045, JBJ-02-112-05 and JBJ-04-125-02 to inhibit EGFR phosphorylation using Ba/F3 (Fig. 2B) and NIH-3T3 (Supplementary Fig. S1B) cells by Western blotting. All three compounds demonstrated mutant selectivity by inhibiting mutant EGFR and downstream AKT and ERK1/2 phosphorylation, but JBJ-04-125-02 was, again, the most potent of all three inhibitors, consistent with the cell proliferation assays (Fig. 2A). We further examined the efficacy of JBJ-04-125-02 in Ba/F3 cells containing the L858R/C797S mutations (Supplementary Fig. S1C). Although JBJ-04-125-02 could inhibit the phosphorylation of EGFR as well as gefitinib, it was not as potent as gefitinib in inhibiting cell proliferation (Supplementary Fig. S1C).

On the basis of the single-agent activity *in vitro*, we sought to determine whether JBJ-04-125-02 could also be effective *in vivo*. JBJ-04-125-02 exhibited a moderate half-life of 3 hours and a high area under curve of 728,577 min·ng/mL (AUC_{last}) following 3 mg/kg intravenous (i.v.) dose. A 20 mg/kg oral dose of JBJ-04-125-02 achieved an average maximal plasma concentration of 1.1 μmol/L with an oral bioavailability of only 3% (Supplementary Table S3A). On the basis of these findings, we performed a pharmacodynamic study whereby $EGFR^{L858R/T790M/C797S}$ genetically engineered mice (GEM), following tumor development, were treated with 3 doses of either vehicle, 100 mg/kg of JBJ-02-112-05, or 50 mg/kg or 100 mg/kg of JBJ-04-125-02 by oral gavage administered once daily, and evaluated the effects on phosphorylation of EGFR and downstream signaling (Fig. 2C). Both the 50 mg/kg and the 100 mg/kg doses effectively inhibited phosphorylation of EGFR, AKT, and ERK1/2 (Fig. 2C). JBJ-02-112-05 (at 100 mg/kg) also inhibited phosphorylation of EGFR and downstream signaling pathways, although not as robustly as JBJ-04-125-02 (Fig. 2C). In a subsequent efficacy study, we treated $EGFR^{L858R/T790M/C797S}$ GEMs with vehicle, 100 mg/kg of JBJ-02-112-05, or 50 mg/kg

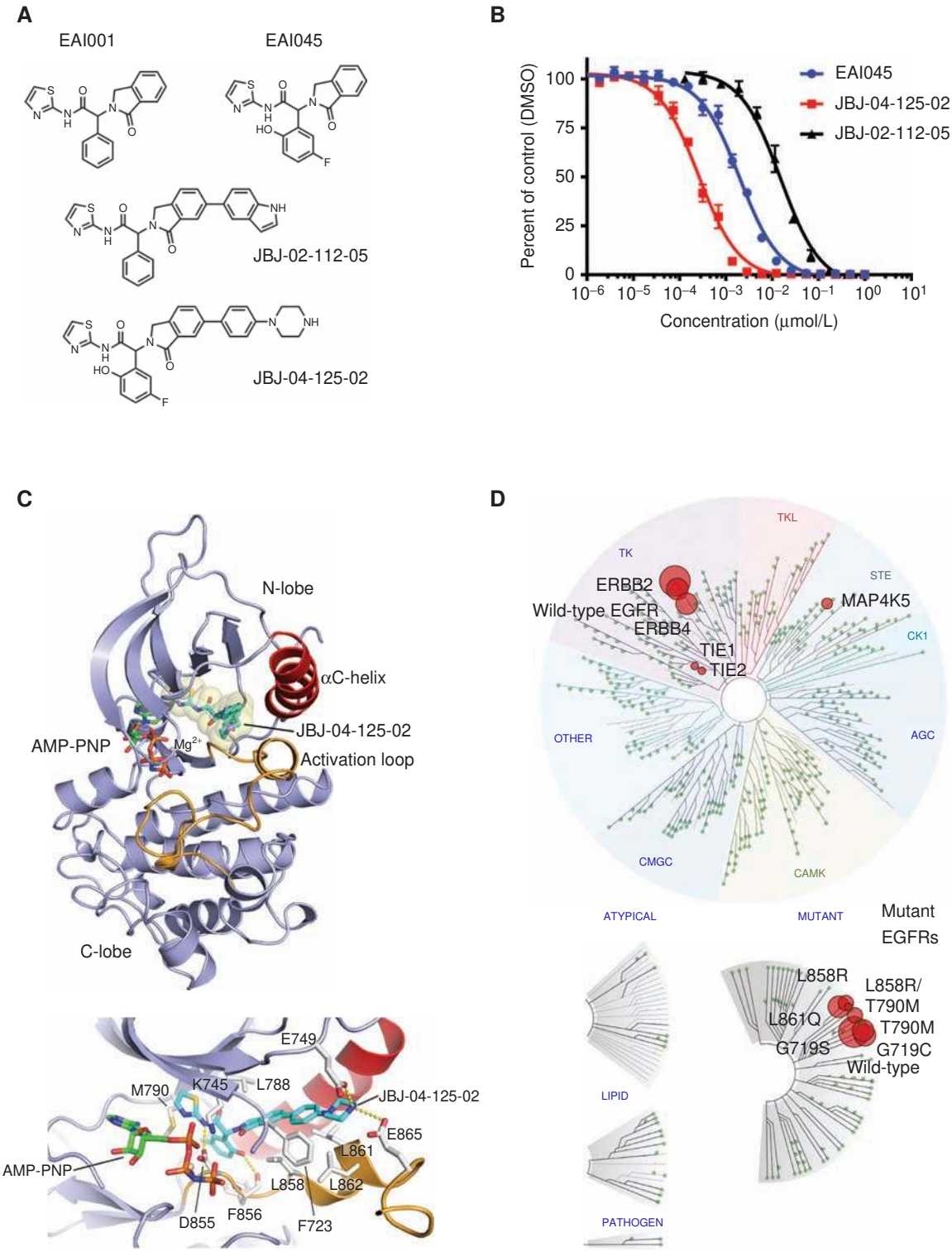

Figure 1. Structural properties and biochemical analyses of the allosteric inhibitor JBJ-04-125-02. **A,** Molecular structures of EAI001, EAI045, JBJ-02-112-05, and JBJ-04-125-02. **B,** *In vitro* inhibition of $EGFR^{L858R/T790M}$ kinase by allosteric inhibitors. Enzyme activity was measured using a homogeneous time-resolved fluorescence–based assay in the presence of increasing concentrations of each inhibitor as indicated. Fractional activity is relative to a 1% DMSO control. **C,** Crystal structure of $EGFR^{T790M/V948R}$ bound to JBJ-04-125-02 and AMP-PNP. JBJ-04-125-02 is displayed using CPK-coloring with cyan carbon atoms. Distinct hydrogen bonds are shown as a dashed line. **D,** Kinome selectivity obtained from KINOME*scan* (DiscoverX) using 10 μmol/L of JBJ-04-125-02 against 468 kinases. The size of circles mapped onto the kinase phylogenetic tree utilizing DiscoverX TREEspot corresponds to the strength of the binding affinity as indicated in the figure. S-score [35] indicates the relative selectivity of the compound with 35% cutoff (number of nonmutant kinases with <35% control/number of nonmutant kinases tested).

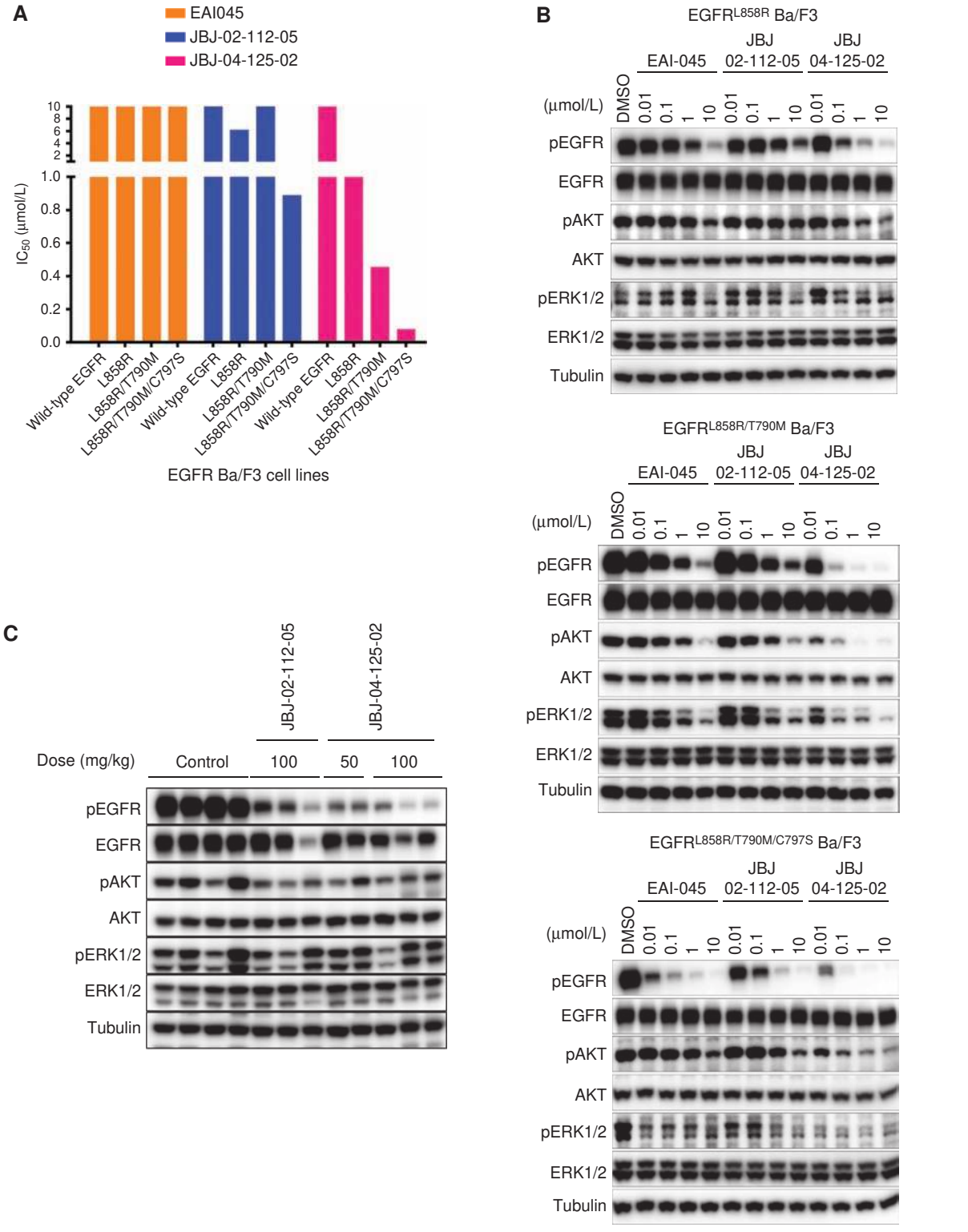

Figure 2. JBJ-04-125-02 is effective *in vitro* and *in vivo* in *EGFR*^{C797S}-containing models. **A,** IC_{50} (μmol/L) of EAI045, JBJ-02-112-05, and JBJ-04-125-02 in Ba/F3 cells stably transfected with EGFR^{L858R}, EGFR$^{L858R/T790M}$, EGFR$^{L858R/T790M/C797S}$ mutations were graphed from a representative experiment that was repeated at least three times. **B,** Western blotting analyses of EGFR activity (phospho-EGFR, EGFR) and downstream signaling (phospho-AKT, AKT, phospho-ERK1/2, ERK1/2) of EGFR^{L858R}, EGFR$^{L858R/T790M}$, EGFR$^{L858R/T790M/C797S}$ Ba/F3 cells treated with increasing concentrations of EAI045, JBJ-02-112-05, and JBJ-04-125-02. **C,** Western blotting analyses of EGFR activity (phospho-EGFR, EGFR) and downstream signaling (phospho-AKT, AKT, phospho-ERK1/2, ERK1/2) in the lung tumor tissues of mice that were dosed with either control, JBJ-02-112-05 (100 mg/kg), or JBJ-04-125-02 (50 mg/kg or 100 mg/kg) for 3 days once daily. Samples were harvested 3 hours after the last dose for analysis. (*continued on following page*)

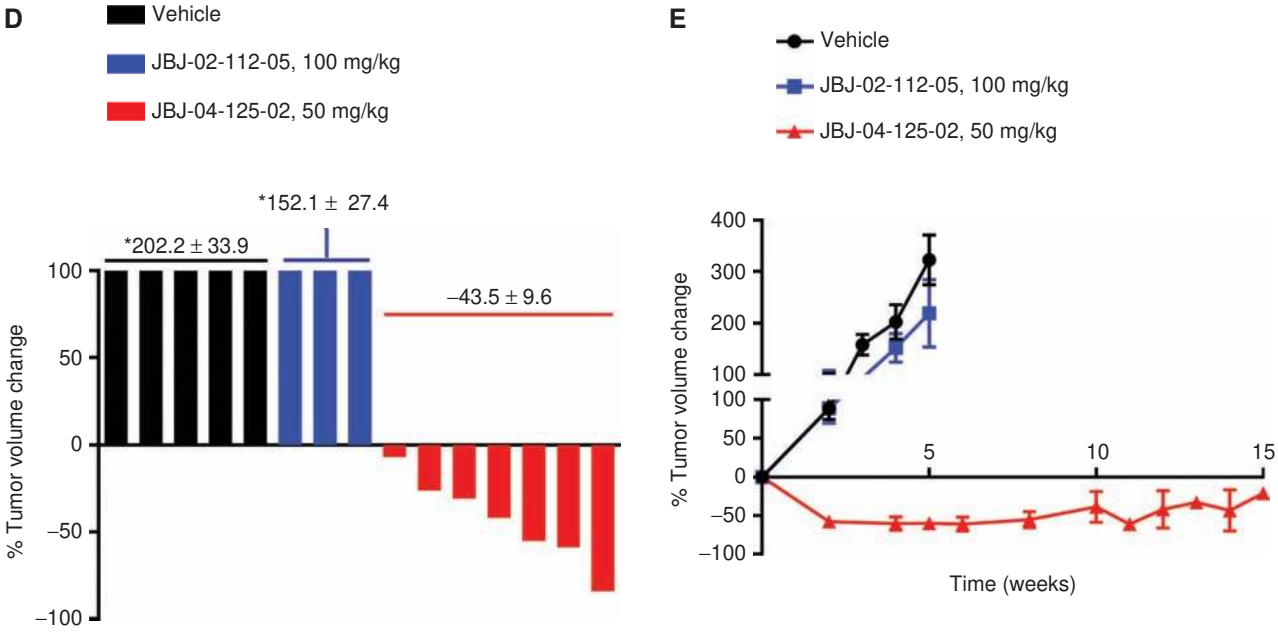

Figure 2. ***(Continued)*** **D,** Waterfall plot indicating the percentage of tumor volume change in mice after 4 weeks of treatment with vehicle ($n = 5$), 100 mg/kg of JBJ-02-112-05 ($n = 3$), or 50 mg/kg of JBJ-04-125-02 ($n = 7$). *For vehicle- and JBJ-02-112-05–treated mice, tumor volumes more than 100% are truncated at 100%. **E,** Efficacy study assessing the percentage of tumor volume change in mice over 15 weeks of treatment with vehicle ($n = 5$), 100 mg/kg of JBJ-02-112-05 ($n = 3$), or 50 mg/kg of JBJ-04-125-02 ($n = 4$). Data points represent the group mean of tumor volume (tumor volume change; %) ± SEM relative to the start of treatment for all available data at the indicated time point (weeks).

of JBJ-04-125-02 and followed the change in tumor volume by serial MRI. Despite the better pharmacokinetic profile of JBJ-02-112-05 (Supplementary Table S3A) compared with JBJ-04-125-02, it was ineffective in the efficacy study and tumor growth was similar to the vehicle control. In contrast, JBJ-04-125-02 treatment led to marked tumor regressions within 4 weeks of treatment (Fig. 2D), which were sustained for 15 weeks of treatment (Fig. 2E). Despite the poor oral bioavailability of JBJ-04-125-02, long-term treatment led to drug accumulation in plasma and tumor, which likely accounted for its efficacy (Supplementary Table S3B). Notably, JBJ-04-125-02 treatment was not associated with weight loss or overt signs of toxicity (Supplementary Fig. S2A and data not shown).

JBJ-04-125-02 Demonstrates Distinct Potency in Human Cancer Cell Lines Harboring *EGFR*$^{L858R/T790M}$ Mutations

H1975 and H3255GR cells are human lung cancer cell lines that possess *EGFR*$^{L858R/T790M}$ mutations (21), but unlike the Ba/F3 cells, they also contain variable copy-number gains in the *EGFR* locus, express other ERBB family members, and are hence more representative of real human cancers. Cell viability assay revealed that JBJ-04-125-02 could inhibit cell proliferation of H1975 cells at low nanomolar concentrations, similar to what was observed with osimertinib treatment (Fig. 3A). Interestingly, JBJ-04-125-02 could downregulate EGFR and ERK1/2 phosphorylation more potently than osimertinib whereas its ability to inhibit AKT phosphorylation was similar to osimertinib (Fig. 3B). We next evaluated whether JBJ-04-125-02 could also inhibit tumor growth *in vivo* using the H1975 xenograft mouse model. A pharmacodynamic study following treatment with JBJ-04-125-02 (3 doses; 100 mg/kg) led to a reduction in EGFR phosphorylation but only subtle changes in AKT and ERK1/2 phosphorylation (Fig. 3C). In contrast, osimertinib treatment (3 doses; 25 mg/kg) led to a complete inhibition of EGFR phosphorylation and, consequently, more effective inhibition of AKT and ERK1/2 phosphorylation (Fig. 3C). In an efficacy study using the H1975 xenografts, osimertinib treatment led to tumor regressions with almost complete tumor inhibition whereas JBJ-04-125-02 treatment led only to tumor stasis and occasional shrinkage in some mice (Fig. 3D). The JBJ-04-125-02 treatment was not associated with any weight loss (Supplementary Fig. S2B). Puzzled by the efficacy differences of JBJ-04-125-02 in the H1975 cells or xenograft model compared with the Ba/F3 cells or the GEM model, we evaluated the cell proliferation and EGFR activity in the H3255GR cells. Surprisingly, although these cells were sensitive to osimertinib, they were resistant to JBJ-04-125-02 (Fig. 4A). Moreover, EGFR, AKT, and ERK1/2 phosphorylation were notably inhibited by JBJ-04-125-02 only at concentrations of 1 μmol/L and higher, whereas the inhibitory effects of osimertinib were apparent at 10-fold lower concentrations (Fig. 4B). There are two major differences between the H3255GR and the H1975 cell lines. The H3255GR cells contain a concomitant copy-number gain at the *EGFR* locus and contain a much lower (~3% vs. 50%) relative allelic fraction (RAF) of *EGFR*^{T790M} (21, 22). To determine whether the RAF of *EGFR*^{T790M} could account for the observed differences in

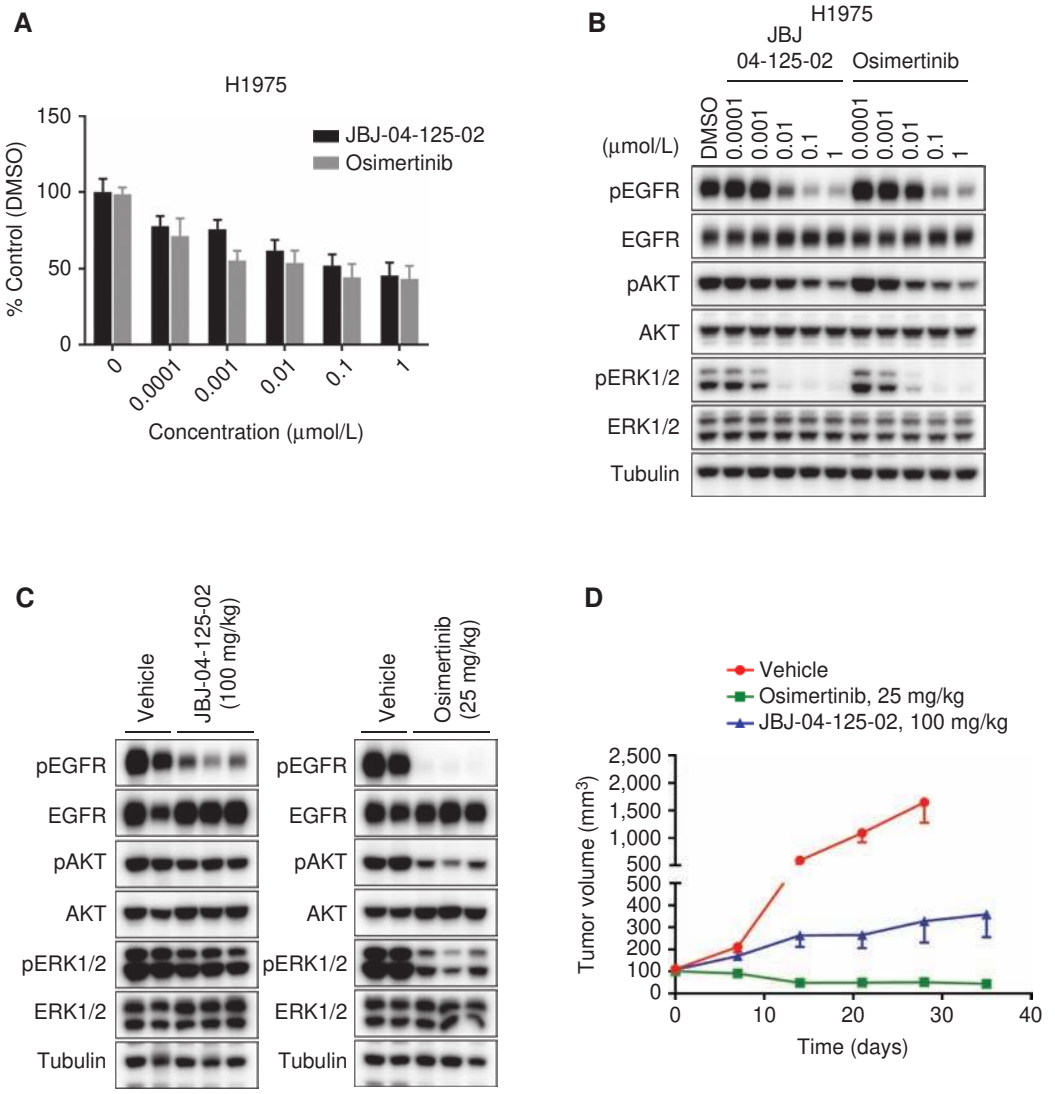

Figure 3. JBJ-04-125-02 inhibits EGFR and downstream signaling and tumor growth in H1975 cells *in vitro* and *in vivo*. **A,** Cell viability assay examining the growth-inhibitory effect of dose-escalated JBJ-04-125-02 and osimertinib in H1975 cells. Data is shown as relative mean compared with control (DMSO; %) ± SD and is a representative graph of at least three independent experiments. **B,** Western blotting analyses of EGFR activity (phospho-EGFR, EGFR) and downstream signaling (phospho-AKT, AKT, phospho-ERK1/2, ERK1/2) in H1975 cells treated with DMSO (as control) or increasing concentrations of JBJ-04-125-02 or osimertinib. **C,** Western blotting analyses of EGFR activity (phospho-EGFR, EGFR) and its downstream signaling (phospho-AKT, AKT, phospho-ERK1/2, ERK1/2) in the lung tumor tissues of mice that were dosed with vehicle, 100 mg/kg of JBJ-04-125-02, or 25 mg/kg of osimertinib for 3 days once daily. Samples were collected 3 hours after the last dose for analysis. **D,** Efficacy study examining the curative effect of vehicle, 25 mg/kg of osimertinib, or 100 mg/kg of JBJ-04-125-02 treatment in mice after tumor development over 35 days. Data are shown as a group mean of tumor volume ± SEM relative to the start of treatment (tumor volume, mm^3) for all available data at the indicated time point (days).

the cell lines, we evaluated both osimertinib and JBJ-04-125-02 in the H3255DR cells that contain a much higher (45%) RAF of *EGFR*^{T790M} (23). The efficacies of both agents were similar in the H3255DR and H3255GR cells (Supplementary Fig. S3A). We also evaluated whether the relative differences in EGFR expression between the H1975 and H3255GR cells could account for the efficacy differences observed in these cell lines. In our prior studies, we demonstrated that EAI045 lacked cellular potency because it could not bind the allosteric site on the receiver subunit of EGFR as this was blocked by the activator subunit of EGFR due to EGFR dimerization. We thus compared the relative amounts of EGFR dimers and monomers in the H1975 and H3255GR cells by cross-linking EGFR followed by Western blotting. The relative amount of EGFR dimers was substantially higher in the H3255GR compared with in the H1975 cells (Fig. 4C). To determine whether EGFR dimers in these cells limited the potency of JBJ-04-125-02, we treated H3255GR cells with JBJ-04-125-02 in combination with cetuximab, which disrupts EGFR dimerization. Cetuximab alone (1 μg/mL or 10 μg/mL) had no effect on H3255GR cells (Fig. 4D). However, when combined with JBJ-04-125-02, an increase in the efficacy of JBJ-04-125-02, albeit not to the level of osimertinib, was observed (Fig. 4D). As cetuximab is an EGFR-directed antibody, and as such inhibits

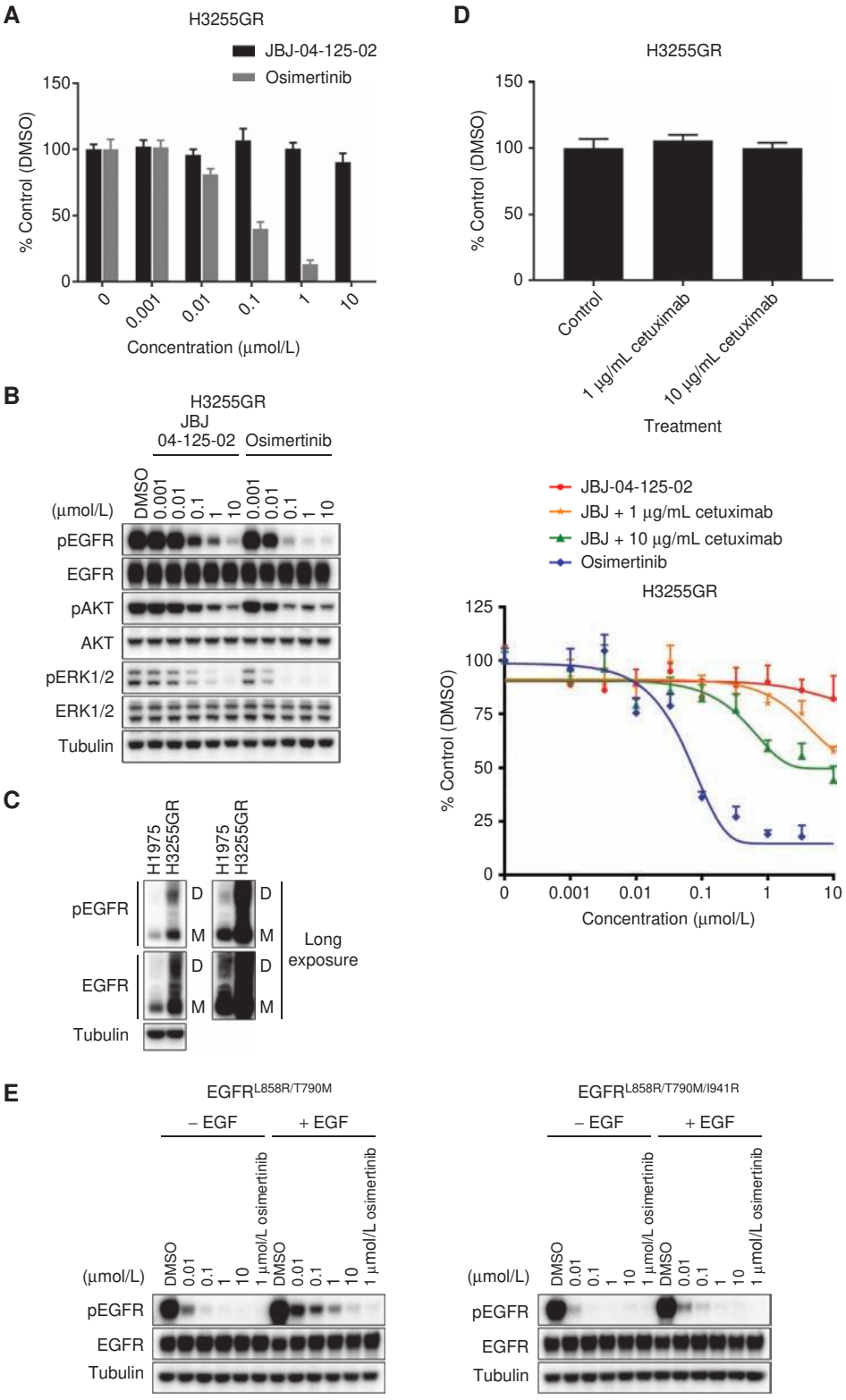

Figure 4. JBJ-04-125-02 and osimertinib have distinct properties in H3255GR cells. **A,** Cell viability assay examining the growth-inhibitory effect of dose-escalated JBJ-04-125-02 and osimertinib in H3255GR cells. Data are shown as relative mean compared with control (DMSO; %) ± SD and the graph is representative of at least three independent experiments. **B,** Western blotting analyses of EGFR activity (phospho-EGFR, EGFR) and its downstream signaling (phospho-AKT, AKT, phospho-ERK1/2, ERK1/2) in H3255GR cells treated with DMSO (as control) or increasing concentrations of JBJ-04-125-02 or osimertinib. Tubulin was used as a loading control for relative protein expression. **C,** Cross-linking study demonstrating the amount of phospho-EGFR and total EGFR monomers (M) and dimers (D) in H1975 versus H3255GR cells. Tubulin was used as a loading control for relative protein expression. **D,** MTS cell viability assay examining the growth-inhibitory effect of control versus 1 μg/mL or 10 μg/mL of cetuximab alone and the effect of dose-escalated JBJ-04-125-02 alone, osimertinib alone, or JBJ-04-125-02 in combination with either 1 μg/mL of cetuximab or 10 μg/mL of cetuximab in H3255GR cells. Data is shown as relative mean compared with control (DMSO; %) ± SD. **E,** Western blot analyses of phospho-EGFR and total EGFR protein expression in EGFR$^{L858R/T790M}$ NIH-3T3 and EGFR$^{L858R/T790M/I941R}$ NIH-3T3 cells treated with DMSO, 1 μmol/L of osimertinib (as controls), or increasing concentrations of JBJ-04-125-02 in the presence or absence of EGF. 10 ng/mL of EGF was added to cells 15 minutes prior to drug treatment. Tubulin was used as a loading control for relative protein expression.

only EGFR dimers, it is possible that dimers with EGFR and other ERBB family members could additionally contribute to these findings. Treatment of EGFR$^{L858R/T790M}$ NIH-3T3 cells with EGF, which induces dimerization, blunted the ability of JBJ-04-125-02 to inhibit EGFR phosphorylation (Fig. 4E). In contrast, EGF treatment had no effect on the ability of JBJ-04-125-02 to inhibit EGFR phosphorylation in the presence of the dimerization-deficient I941R mutation in the EGFR$^{L858R/T790M}$ cells (Fig. 4E; ref. 24). In addition, when treated with EGF, the efficacy and the ability of JBJ-04-125-02 to inhibit cell proliferation and EGFR activity was substantially blunted in the EGFR$^{L858R/T790M}$ Ba/F3 and the H1975 cells, but not in the EGFR$^{L858R/T790M/I941R}$ Ba/F3 cells (Supplementary Fig. S3B and S3C). Collectively, these findings suggest that the presence of EGFR dimers, either as a result of higher levels of EGFR expression or ligand induction, limits the efficacy of JBJ-04-125-02 and likely accounts for the differences in efficacy observed in the Ba/F3 cells, NIH-3T3 cells, and GEMs compared with the human lung cancer cell lines.

Dual Targeting of EGFR with JBJ-04-125-02 and Osimertinib Leads to Enhanced Apoptosis and Delays the Onset of Drug Resistance

Our crystal structure indicates that JBJ-04-125-02 and ATP can bind at the same time to a single mutant EGFR molecule, but the potential for cobinding with various ATP-site inhibitors has not been examined (Fig. 1C). Simple structural modeling suggests that a subset of ATP-site inhibitors, including osimertinib, could bind together with JBJ-04-125-02 (Fig. 5A), but that many should not. In particular, modeling of WZ4002 and anilinoquinazoline-based compounds such as afatinib in the JBJ-04-125-02 cocrystal structure reveals steric clash between the allosteric inhibitor and these ATP-site agents (Supplementary Fig. S4A and S4B). To experimentally probe simultaneous binding of covalent ATP-site inhibitors with JBJ-04-125-02, we generated a biotinylated version of JBJ-04-125-02 for pulldown experiments (Supplementary Fig. S4C). Purified EGFR$^{L858R/T790M}$ protein or EGFR$^{L858R/T790M}$ protein that was pretreated with osimertinib were incubated with biotinylated JBJ-04-125-02 or with a biotinylated linker control followed by precipitation with streptavidin agarose beads and analysis using SDS-PAGE. Biotinylated JBJ-04-125-02 efficiently bound both purified proteins (Fig. 5B). We performed similar studies *in vitro* using EGFR$^{L858R/T790M}$ Ba/F3 cells that were treated with DMSO or with increasing concentrations of either WZ4002 or osimertinib. EGFR was then affinity-purified using the biotinylated JBJ-04-125-02, followed by examination of EGFR levels by Western blotting. Whereas the WZ4002 treatment led to a dose-dependent inhibition of JBJ-04-125-02 binding (as evidenced by a dose-dependent decrease in EGFR precipitation), osimertinib treatment substantially increased the amount of total EGFR associated with JBJ-04-125-02 compared with DMSO control in a dose-independent manner (Fig. 5C). Consistent with structural modeling (Supplementary Fig. S4A and S4B), afatinib behaved similarly to WZ4002 by potently blocking the binding of biotinylated JBJ-04-125-02 (Supplementary Fig. S4D). To determine whether osimertinib treatment led to an increase in the available EGFR monomers for JBJ-04-125-02 binding and, as such, resulted in increased levels of total EGFR in the assay, we performed the same experiment using the dimerization-deficient EGFR$^{L858R/T790M/I941R}$ NIH-3T3 cells. Osimertinib pretreatment led to a similar substantial increase in the amount of total EGFR associated with JBJ-04-125-02 regardless of whether dimerization was functional or deficient in these cells (Fig. 5D). The same enhanced association of JBJ-04-125-02 to EGFR in the presence of osimertinib was also observed in the H3255GR cells (Fig. 5E). These results suggest that among the covalent EGFR inhibitors tested, osimertinib is uniquely able to cobind to mutant EGFR with JBJ-04-125-02. In addition, the binding of JBJ-04-125-02 to EGFR is enhanced in the presence of osimertinib, a phenomenon that is independent of the amount of available EGFR monomers present in the cells.

Given these findings, we next explored whether the combination of osimertinib and JBJ-04-125-02 was more effective than either agent alone in inhibiting proliferation of H3255GR cells. In a cell viability assay, the addition of 10 μmol/L of JBJ-04-125-02 to osimertinib shifted the dose–response curve to the left, suggesting that the combination could increase the potency of osimertinib (Fig. 6A). To determine whether the two-drug combination could lead to an increase in apoptosis compared with either agent alone, we incubated the H3255GR cells with a caspase-3/7 fluorescence dye and followed the apoptosis activity of the cells over time using the IncuCyte Live-Cell fluorescence microscopy analysis system. Although 0.1 μmol/L osimertinib induced the expected time-dependent increase in apoptosis (Fig. 6B; *, $P < 0.001$ vs. DMSO), 10 μmol/L of JBJ-04-125-02 was no more effective than DMSO, consistent with the short-term proliferation assay (Fig. 6A). However, the combination of osimertinib and JBJ-04-125-02 led to a significant increase in apoptosis (Fig. 6B; *, $P < 0.001$ combination treatment vs. DMSO, JBJ-04-125-02 alone or osimertinib alone). We also observed a further inhibition of EGFR, AKT, and ERK1/2 phosphorylation in cells treated with osimertinib in the presence of 1 μmol/L or 10 μmol/L of JBJ-04-125-02 compared with osimertinib treatment alone (Fig. 6C). Intrigued by the observations with JBJ-04-125-02 and osimertinib, we examined whether an earlier-generation allosteric inhibitor, EAI045, possessed the same ability to cobind and enhance EGFR binding following osimertinib treatment. Using an analogous biotinylated pull-down assay, EAI045 did indeed cobind with osimertinib and increase EGFR precipitation (Supplementary Fig. S4E). However, in contrast to JBJ-04-125-02 and osimertinib, the combination of osimertinib and EAI045 was no more effective than osimertinib alone (Supplementary Fig. S4F). Consistent with these observations, there was no increase in apoptosis or in the ability to inhibit EGFR, AKT, or ERK 1/2 phosphorylation in cells treated with the combination of osimertinib and EAI045 compared with osimertinib alone (Supplementary Fig. S4G and S4H). Thus, although osimertinib can cobind with either JBJ-04-125-02 or EAI045 and enhance EGFR precipitation, only the combination of osimertinib and JBJ-04-125-02 can uniquely enhance the efficacy of osimertinib.

We next evaluated the potential therapeutic effects of the dual EGFR inhibitor combination using complementary assays. We first used *N*-ethyl-*N*-nitrosourea (ENU) mutagenesis assay to evaluate the emergence of drug-resistant colonies. We used both EGFR^{L858R}- and EGFR$^{L858R/T790M}$-containing

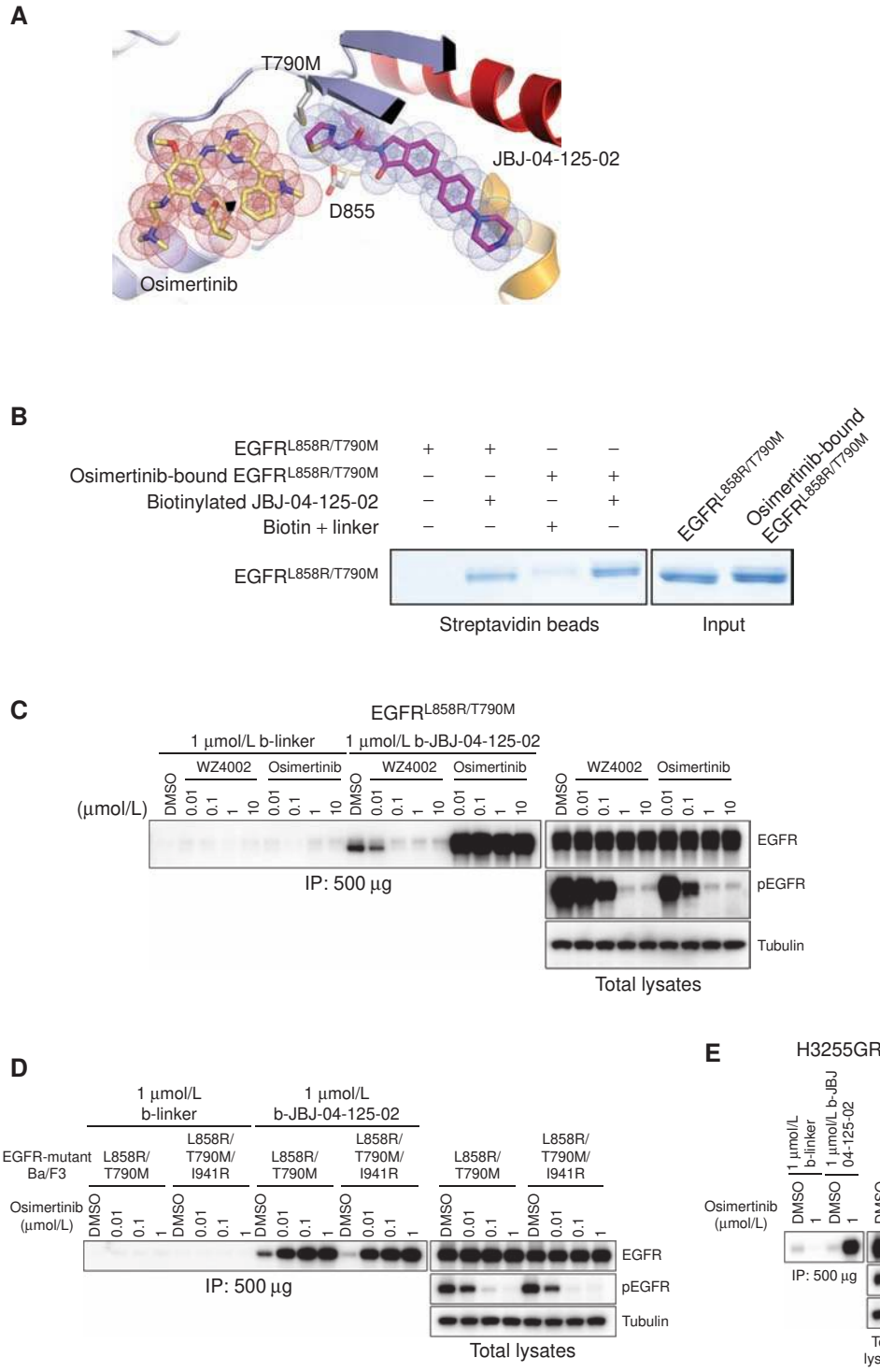

Figure 5. Osimertinib can cobind with JBJ-04-125-02 to mutant EGFR. **A,** Modeling of osimertinib in the JBJ-04-125-02 cocrystal structure. Schematic depicting osimertinib and JBJ-04-125-02 binding site. **B,** SDS-PAGE analyses of EGFR$^{L858R/T790M}$ using purified EGFR$^{L858R/T790M}$ protein and purified EGFR$^{L858R/T790M}$ protein that was preincubated and covalently bound to osimertinib followed by precipitation with biotinylated linker or biotinylated JBJ-04-125-02. **C,** Western blot analyses of EGFR protein in EGFR$^{L858R/T790M}$ Ba/F3 cells pretreated with increasing concentrations of WZ4002 or osimertinib followed by precipitation of EGFR using biotinylated (b) linker (as control) or biotinylated JBJ-04-125-02. Both phospho-EGFR and total EGFR protein expression was assessed to ensure that the activity of the drugs and EGFR protein were present in the lysates. **D,** Western blot analyses of EGFR protein expression in EGFR$^{L858R/T790M}$ and EGFR$^{L858R/T790M/I941R}$ Ba/F3 cells were performed as described in **C** with cells pretreated with increasing concentrations of osimertinib. **E,** Western blot analyses of EGFR protein expression in H3255GR cells were performed as described in **C** with cells pretreated with either DMSO or 1 μmol/L of osimertinib.

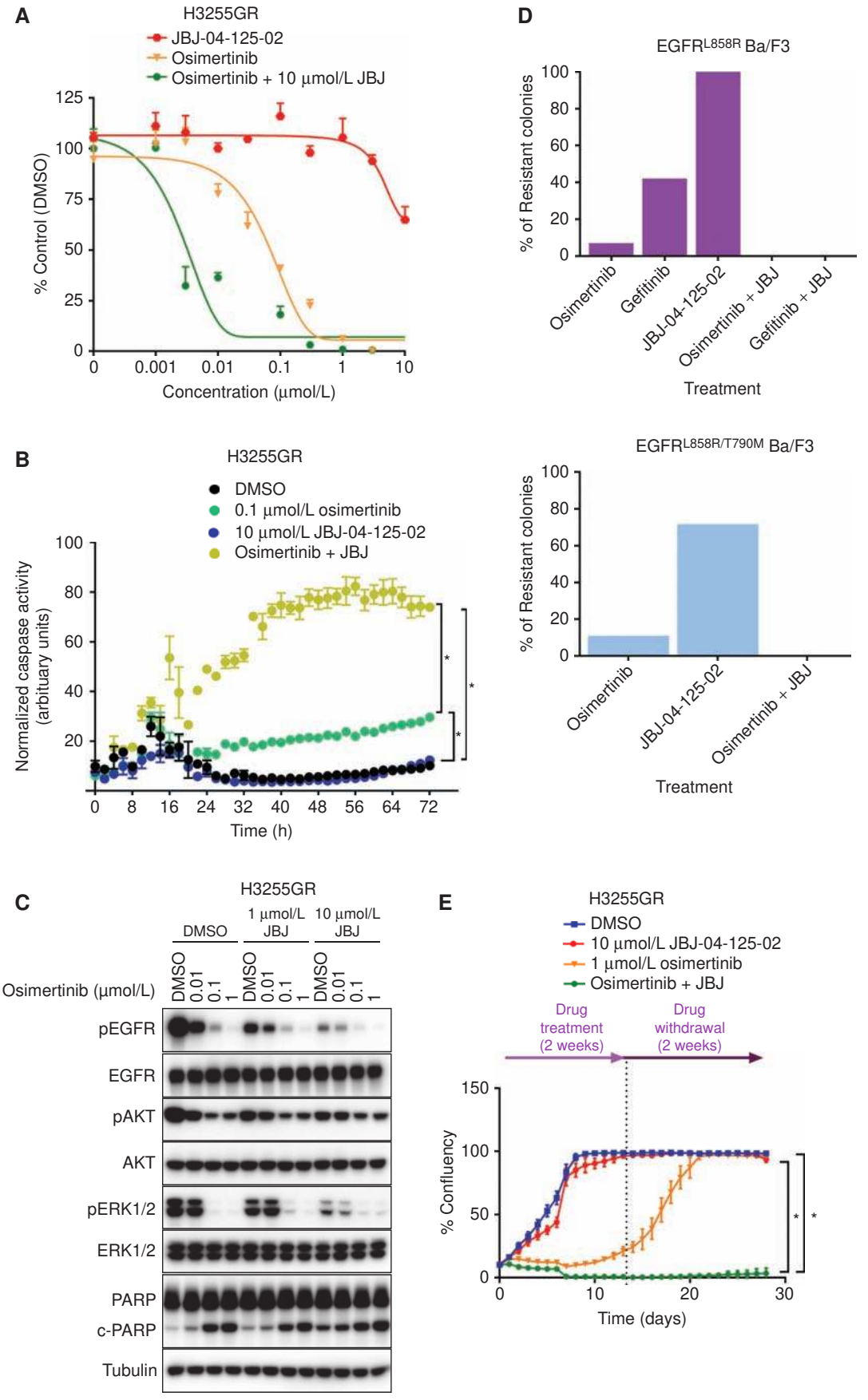

Ba/F3 cells and, following ENU exposure, selected colonies resistant to 1 μmol/L ATP-competitive EGFR inhibitors (gefitinib or osimertinib), 10 μmol/L JBJ-04-125-02, or the combination of both types of inhibitors. In the $EGFR^{L858R}$ Ba/F3 cells, we isolated resistant colonies following selection with gefitinib alone (42%), osimertinib alone (7%) or JBJ-04-125-02 alone (100%; Fig. 6D). In contrast, no resistant colonies were isolated from the gefitinib/JBJ-04-125-02 or the osimertinib/JBJ-04-125-02 combination (Fig. 6D). Similarly, using the $EGFR^{L858R/T790M}$ Ba/F3 cells, 11% of osimertinib colonies and 72% of JBJ-04-125-02 colonies emerged while no resistant colonies were isolated from the osimertinib/JBJ-04-125-02–treated cells following ENU exposure (Fig. 6D). We next performed a long-term *in vitro* treatment assay where H3255GR cells were treated with osimertinib alone (1 μmol/L), JBJ-04-125-02 alone (10 μmol/L), or the combination of both agents for 2 weeks followed by drug withdrawal for another 2 weeks. At the 2-week time point, vehicle and JBJ-04-125-02–treated cells reached full confluency (Fig. 6E). In contrast, osimertinib treatment, although initially effective, resulted in the development of resistance. At 2 weeks, cells reached 24% confluency, with 96% confluency achieved by 28 days (Fig. 6E). However, the combination of osimertinib/JBJ-04-125-02 led to a significant reduction in cell confluency (0.3% at 2 weeks; $P \leq 0.0001$ combination treatment vs. DMSO and JBJ-04-125-02 alone). Notably, cells treated with osimertinib/JBJ-04-125-02 were only 4% confluent after drugs were withdrawn for two weeks (*, $P < 0.0001$ combination treatment vs. DMSO, osimertinib alone, and JBJ-04-125-02 alone).

As the combination of JBJ-04-125-02 and osimertinib could sensitize previously resistant H3255GR cells, we next sought to determine whether this same combination treatment could delay emergence of resistance in H1975 cells, which are partially sensitive to JBJ-04-125-02 both *in vitro* and *in vivo*. Similar to the results from the Ba/F3 and H3255GR cells (Fig. 5C and E), pretreatment with osimertinib also enhanced the association of EGFR with biotinylated JBJ-04-125-02 in H1975 cells (Fig. 7A). In the long-term *in vitro* assay, cells treated with osimertinib alone and JBJ-04-125-02 alone were fully confluent respectively at the end of the study (Fig. 7B). However, cells that were treated with the JBJ-04-125-02/osimertinib combination had a much slower regrowth rate after drug withdrawal with a confluency of 20% at the end of the 4-week study (*, $P < 0.0001$ combination treatment vs. DMSO, osimertinib alone, and JBJ-04-125-02 alone; Fig. 7B). We further examined whether the two-drug combination would also be effective *in vivo*. In a 2-week treatment of non–tumor-bearing mice with both JBJ-04-125-02 (100 mg/kg) and osimertinib (25 mg/kg), we observed no evidence of weight loss, changes in serum chemistries, blood counts, or end organ toxicity (Supplementary Fig. S5A and S5B). Initially, we treated tumor-bearing H1975 xenografts with vehicle, 100 mg/kg of JBJ-04-125-02 alone, 25 mg/kg of osimertinib alone, or the combination of both drugs for 28 days followed by drug withdrawal. However, in both mice treated with osimertinib alone or in combination with JBJ-04-125-02, we achieved close to 100% tumor regression, and thus were not able to fully evaluate the differences between these treatments (Supplementary Fig. S5C). Therefore, we performed a subsequent *in vivo* study using the same dose of JBJ-04-125-02 (100 mg/kg) combined with a lower, but *in vivo* effective, dose (2.5 mg/kg) of osimertinib (10). Treatment with either 2.5 mg/kg of osimertinib or 100 mg/kg of JBJ-04-125-02 led to a minimal reduction in tumor volume at day 18 in only a subset of treated mice (Fig. 7C). However, treatment with the combination of both drugs led to substantial tumor regressions in all mice (Fig. 7C). Furthermore, mice treated with the osimertinib/JBJ-04-125-02 combination had significantly smaller minimum residual tumors when compared with those treated with either osimertinib or JBJ-04-125-02 alone (*, $P < 0.001$, combination treatment vs. osimertinib; #, $P = 0.0065$, combination treatment vs. JBJ-04-125-02; Wilcoxon rank sum test; Fig. 7D). Finally, we examined the effect of these 28-day drug treatments on survival for up to 101 days. The median overall survival (OS) among mice treated with vehicle was 19 days (95% CI, 16 days–NA). For mice treated with osimertinib, the median OS was 33.5 days (95% CI: 27–NA) whereas mice treated with JBJ-04-125-02 had a median OS of 37 days (95% CI: 27–NA). Notably, mice treated with combination therapy had a median OS of 74 days (95% CI: 67–NA). The OS distributions were significantly different from one another (log-rank $P < 0.0001$; Fig. 7E). We repeated the *in vivo* study using an erlotinib-resistant patient-derived xenograft (PDX) DFCI282 ($EGFR^{L858R/T790M}$), and observed

Figure 6. The combination of JBJ-04-125-02 and osimertinib is more effective than either single agent alone. **A,** Cell viability assay examining the growth-inhibitory effect of JBJ-04-125-02 alone, osimertinib alone, or osimertinib in combination with 10 μmol/L of JBJ-04-125-02 in H3255GR cells. Data are shown as relative mean compared with control (DMSO; %) ± SD and the graph is representative of at least three independent experiments. **B,** IncuCyte analyses examining the apoptotic effect of DMSO versus 0.1 μmol/L of osimertinib alone, 10 μmol/L JBJ-04-125-02 alone, or the combination of both compounds in H3255GR cells. Data were normalized by dividing the average fluorescence objects per well by the percentage of confluency at each timepoint and were shown as the normalized caspase activity (arbituary units) ± SEM over time. Figure is a representative graph of at least three independent experiments. The means of treatment groups were compared using a one-way ANOVA with a Tukey *post hoc* test; *, $P < 0.001$, DMSO, or JBJ-04-125-02 or osimertinib versus combination treatment. **C,** Western blot analyses of EGFR activity (phospho-EGFR, EGFR) and downstream signaling (phospho-AKT, AKT, phospho-ERK1/2, ERK1/2, PARP, and cPARP) in H3255GR cells treated with increasing concentrations of osimertinib as a single agent (DMSO) or in combination with either 1 μmol/L or 10 μmol/L JBJ-04-125-02 (JBJ). Tubulin was used as a loading control for relative protein expression. Figure is a representative of three independent experiments. **D,** Quantitative analyses of resistant colonies that emerged after continuous treatment with 1 μmol/L of osimertinib alone, 1 μmol/L of gefitinib alone, 10 μmol/L of JBJ-04-125-02 alone, or JBJ-04-125-02 in combination with either osimertinib or gefitinib for at least four weeks in ENU-treated $EGFR^{L858R}$ and $EGFR^{L858R/T790M}$ Ba/F3 cells. Data is shown as the percentage (%) of resistant colonies relative to the total number of colonies (300) that underwent indicated treatments. Figure is a representative of at least three independent experiments. **E,** IncuCyte analyses assessing the rate at which H3255GR cells achieve confluency when they are treated with DMSO, 1 μmol/L of osimertinib, 10 μmol/L JBJ-04-125-02 alone, or osimertinib and JBJ in combination for two weeks followed by drug washout and withdrawal for two weeks. Data is shown as the percentage (%) of confluency over time and is a representative graph of at least three independent experiments. The means of treatment groups were compared using a one-way ANOVA with a Tukey *post hoc* test; *, $P \leq 0.0001$, DMSO versus osimertinib or combination treatment, osimertinib versus JBJ-04-125-02 or combination treatment, JBJ-04-125-02 versus combination treatment.

a similar trend. The combination treatment reduced tumor volume to a greater extent than vehicle or when the compounds were given as a single agent (Wilcoxon rank sum test; $P = 0.065$; Fig. 7F). Collectively, both *in vitro* and *in vivo* studies suggest that the combination of osimertinib and JBJ-04-125-02 is a significantly more effective treatment approach than either agent alone.

DISCUSSION

Single-agent targeted therapies, including EGFR inhibitors in *EGFR*-mutant lung cancer, are clinically effective in the right patient population but seldom, if ever, lead to long-term benefits or cures of advanced cancers (4, 5). Osimertinib, a mutant-selective EGFR inhibitor, is effective both in patients with NSCLC who have developed $EGFR^{T790M}$-mediated resistance to prior EGFR inhibitors and in EGFR TKI–naïve patients, but is limited by the development of acquired drug resistance, including the C797S mutation (13, 15–17). *In vitro* and limited patient studies suggest that cancers with $EGFR^{C797S}$ following first-line osimertinib treatment (L858R/C797S or Del_19/C797S) remain sensitive to a quinazoline-based EGFR inhibitor, but T790M will inevitably occur as part of a drug-resistance mechanism (25, 26). Therefore, even though the sequence of mutation occurrence may differ from patients who received gefitinib/erlotinib compared with osimertinib as first-line therapy, both patient populations are expected to ultimately develop the same three mutations that render their cancer untreatable by all currently available TKIs. Concomitant strategies, aimed at inhibiting either the target itself and/or a critical downstream signaling pathway, are approaches that could translate into improved patient outcomes. Compelling clinical examples to date include the combination of trastuzumab and pertuzumab or the combination of dabrafenib and trametinib, both of which lead to improved survivals in *HER2*-positive breast cancer and in $BRAF^{V600E}$-mutant melanoma, respectively (27, 28).

Here, we identify and study a next-generation L858R-specific mutant-selective allosteric EGFR inhibitor, JBJ-04-125-02, which has single-agent activity *in vitro* and *in vivo*; in contrast to the first-generation allosteric EGFR inhibitor EAI045. However, the efficacy is not universally observed in all *EGFR*-mutant models, including H1975 and H3255GR human lung cancer cell lines. These cells contain concomitant copy-number changes in *EGFR* and express other ERBB family members and/or EGFR family ligands, all of which are characteristics found in *EGFR*-mutant lung cancers (29, 30). A common feature limiting the efficacy of JBJ-04-125-02 was the presence of higher levels of EGFR dimers due to increased expression of EGFR itself or mediated by EGFR ligands (Fig. 4C and E; Supplementary Fig. S3B and S3C). The allosteric mechanism of JBJ-04-125-02 antagonizes dimer formation, as shown by the inactive conformation of the cocrystal structure and by its single-agent inhibitory activity in Ba/F3 cell and GEM models. However, via the same mechanism, dimerization must antagonize binding of the allosteric inhibitor. Thus, our findings suggest that there is likely a threshold, observed at lower levels of EGFR expression or in the absence of EGFR ligand expression as in the Ba/F3 cells and GEM models, below which dimer formation seldom takes place (or is a minority population as observed in H1975 cells; Fig. 4C), and in such cases JBJ-04-125-02 remains effective. Above this threshold, and/or in the presence of a substantial fraction of dimers, JBJ-04-125-02 is not able to effectively inhibit EGFR. Thus, these studies provide important insight as to how we can further optimize an allosteric inhibitor to be efficacious for all *EGFR*-mutant lung cancers. Our studies also highlight the importance of extending preclinical studies beyond simple model systems for drug development, because human cancers are more complex and thus may contribute to differences in drug efficacy.

Remarkably, we observed a unique enhancement of JBJ-04-125-02 binding to mutant EGFR in the presence of osimertinib (Figs. 5C and E and 7A). This is not a feature of all covalent ATP-competitive EGFR inhibitors including WZ4002 or afatinib (Fig. 5C; Supplementary Fig. S4A, S4B, and S4D). However, the ability of an allosteric inhibitor and a tyrosine kinase to cobind to a single mutant EGFR molecule does not necessarily translate to an increase in the

Figure 7. The combination of JBJ-04-125-02 and osimertinib delays the emergence of resistance *in vitro* and *in vivo* in H1975 cells. **A,** Western blot analyses of EGFR protein expression in H1975 cells pretreated with DMSO or 1 μmol/L of osimertinib followed by precipitation of EGFR using biotinylated linker or biotinylated JBJ-04-125-02. Both phospho-EGFR and total EGFR protein expression was assessed to ensure that the activity of the drugs and EGFR protein were present in the lysates. Tubulin was used as a loading control for relative protein expression. Figure is representative of three independent experiments. **B,** IncuCyte analyses assessing the rate at which H1975 cells achieve confluency when they are treated with DMSO, 1 μmol/L of osimertinib, 10 μmol/L JBJ-04-125-02 alone, or the two-drug combination for two weeks followed by drug washout and withdrawal for two weeks. Data are shown as the percentage of confluency over time and the graph is representative of at least three independent experiments. The means of treatment groups were compared using a one-way ANOVA with a Tukey *post hoc* test; *, $P \leq 0.0001$, DMSO versus osimertinib or combination treatment, osimertinib versus JBJ-04-125-02 or combination treatment, JBJ-04-125-02 versus combination treatment. **C,** Waterfall plot indicating the percentage of tumor volume change at 18 days in H1975 xenograft mice treated with vehicle ($n = 8$), 2.5 mg/kg of osimertinib ($n = 8$), 100 mg/kg of JBJ-04-125-02 ($n = 7$), and combination of osimertinib and JBJ-04-125-02 ($n = 8$). *For vehicle- and osimertinib-treated mice, tumor volumes above 100% are truncated at 100%. **D,** Minimum residual tumor size (mm^3) was recorded for each individual mouse in each treatment group described in **C** as a scatter plot. The treatment groups were compared using a Wilcoxon rank sum test; *, $P < 0.001$, combination treatment versus osimertinib; #, $P = 0.0065$, combination treatment versus JBJ-04-125-02. **E,** Kaplan–Meier survival curves of H1975 xenograft mice from each treatment group described in **C** over time (days). The overall survival distribution was compared using a log-rank (Mantel–Cox) test and were significantly different from one another; log-rank $P < 0.0001$. **F,** Efficacy study examining the effect of vehicle, 2.5 mg/kg of osimertinib, or 100 mg/kg of JBJ-04-125-02 treatment or combination treatment in DFCI282 xenograft mice after tumor development over 31 days. Data is shown as a group mean of tumor volume ± SEM relative to the start of treatment (tumor volume, log mm^3) for all available data at the indicated time point (days).

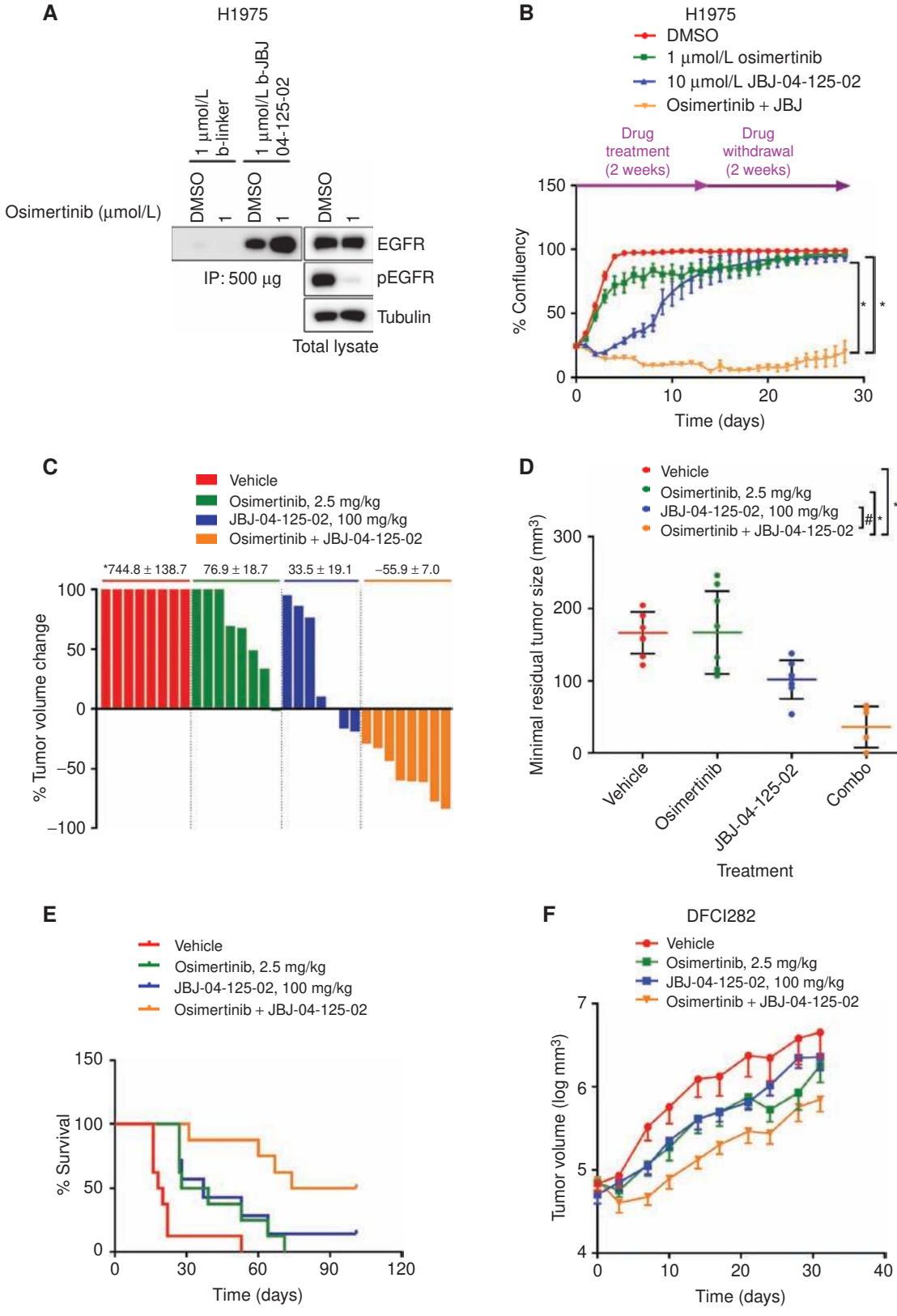

potency of the combination. EAI045, a less potent allosteric inhibitor, can also cobind with osimertinib, but the combination was no more efficacious than osimertinib alone (Supplementary Fig. S4E–S4H). The unique mechanism whereby osimertinib enhances the binding ability of JBJ-04-125-02 and results in enhanced efficacy of the combination is not fully understood. It is possible that in the presence of osimertinib, the ability of JBJ-04-125-02 to access the allosteric site is enhanced or the affinity for the mutant receptor increases. Regardless, this unique interaction of the two drugs enhances the efficacy of osimertinib in two independent ways, which has potential clinical implications. First, in the presence of both drugs, we are unable to recover EGFR mutants that mediate drug resistance (Fig. 6D). Thus, a combination of osimertinib and JBJ-04-125-02 could limit the emergence of *EGFR* mutations as a resistance mechanism, regardless of whether osimertinib is clinically used in EGFR treatment–naïve or $EGFR^{T790M}$ patients, and as such lead to a delay in the emergence of drug resistance. Second, JBJ-04-125-02 enhances the potency of osimertinib by inducing a greater degree of apoptosis and a significant improvement in efficacy (Fig. 6B). The delay in drug resistance *in vitro* and/or tumor regrowth *in vivo* observed in the combination treatment group translates to increased survival *in vivo* in the H1975 model (Fig. 7E). Unlike cetuximab, osimertinib is a mutant-selective EGFR inhibitor, and thus the combined treatment of JBJ-04-125-02 with osimertinib is likely to lead to less toxicity and a wider therapeutic index compared with the cetuximab combination.

Combinations of small-molecule inhibitors against the same target have previously been evaluated in preclinical studies. Recent studies demonstrate that GNF-5 and asciminib (ABL001), allosteric ABL1 inhibitors that bind to the myristoyl binding pocket, are able to overcome resistance mutations to the ATP-competitive ABL1 inhibitor nilotinib and vice versa (31, 32). Combination therapy with both agents administered simultaneously was highly effective and led to complete tumor eradication (31). Analogously, two ATP-competitive EGFR kinase inhibitors, gefitinib and osimertinib, can each overcome resistance mutations to the other agent, but when used together entirely limit the emergence of resistance mechanisms mediated by an *EGFR* mutation (25). In the former example, both agents can bind a single BCR–ABL1 molecule at the same time, whereas in the latter this is not possible. However, in neither example, unlike in this study, does the binding of one agent uniquely enhance the binding of the other agent.

In summary, we identify a single-agent mutant-selective allosteric EGFR inhibitor, JBJ-04-125-02. Although it is effective *in vitro* and *in vivo*, there are still limitations to this approach. The identification of JBJ-04-125-02 serves as an important proof of concept to demonstrate the feasibility of developing a single-agent mutant-selective allosteric EGFR inhibitor. Current efforts should focus on developing an allosteric inhibitor that can ideally target not only L858R but also the Del_19 mutation. However, because the allosteric pocket in which JBJ-04-125-02 and previous allosteric inhibitors bind is uniquely formed in the presence of the L858R mutation, it remains a challenge to develop an allosteric inhibitor that could simultaneously inhibit both mutant forms of EGFR. Intriguingly, although osimertinib is more effective than gefitinib or erlotinib in EGFR TKI–naïve patients, it is disproportionally more effective in patients with *EGFR* exon 19 deletions (median PFS 21.4 vs. 11 months) compared with those with an L858R mutation (median PFS 14.4 vs. 9.5 months), suggesting a need to continue to develop new therapeutic approaches specifically for patients with $EGFR^{L858R}$-mutant NSCLC (15). The greatest therapeutic potential of JBJ-04-125-02 is observed when it is combined with osimertinib, and as such the two-drug combination could potentially lead to enhanced clinical benefits beyond those currently achievable with single-agent osimertinib in patients with $EGFR^{L858R}$-mutant lung cancer.

METHODS

Cell Lines and Drug Compounds

The EGFR-mutant NSCLC cell line H1975 was purchased from the ATCC (CRL5908). Ba/F3 cells were a generous gift from the laboratory of Dr. David Weinstock (in 2014). Wild-type EGFR, mutant EGFR Ba/F3 cells, and NIH-3T3 cells were generated and characterized as described previously (9, 18). H1975, Ba/F3, and NIH-3T3 cells were cultured as described previously (9, 25). H3255GR and H3255DR were cultured in ACL-4 media (21, 23). All human cancer cells were authenticated in May 2017 using the Promega GenePrint 10 System at the RTSF Research Technology Support Facility in the Genomic Core Laboratory, Michigan State University (East Lansing, MI). All murine mutant Ba/F3 and NIH-3T3 cells were not authenticated because their short tandem repeat profile has not been made publicly available, but they were sequenced to ensure they possess the correct mutations. All cell lines were tested negative for *Mycoplasma* using the Mycoplasma Plus PCR Primer Set (Agilent). All cell lines were passaged and used for no longer than 4 weeks before new cells with similar passage numbers were thawed for all described experiments. Osimertinib (HY-15772) and WZ4002 (HY-12026) were purchased from Medchem Express. Gefitinib (S1025) and afatinib (S1011) were purchased from Selleck Chemicals. EAI045 and EAI001 were synthesized according to previously published methods (18). JBJ-02-112-05, JBJ-04-125-02, biotin-conjugated linker, biotin-conjugated JBJ-04-125-02, and biotinylated EAI045 were synthesized as described in the Supplementary Methods.

EGFR Protein Expression and Purification

Constructs spanning residues 696–1022 of human EGFR (including wild-type, L858R/T790M, L858R/T790M/C797S, and T790M/V948R mutant sequences) were prepared in a His_6 and GST-fusion double-tagged format using the pTriEX system (Novagen) for expression in Sf9 insect cells essentially as described previously (8, 33). EGFR kinase proteins were purified by Ni-NTA and glutathione-affinity chromatography, followed by size-exclusion chromatography after cleavage with TEV to remove the His_6-GST fusion partner following established procedures (8, 33).

HTRF-Based EGFR Biochemical Assays

Biochemical assays with $EGFR^{L858R/T790M}$ were carried out using a homogeneous time-resolved fluorescence (HTRF) KinEASE-TK (Cisbio) assay as described previously (34) at the ICCB Longwood Screening Facility at Harvard Medical School (Boston, MA). Assays were performed with enzyme concentration of 20 pmol/L and 100 μmol/L ATP. Inhibitor compounds in DMSO were dispensed directly into 384-well plates with the D300 Digital dispenser (Hewlett Packard) followed immediately by the addition of aqueous buffered solutions using the Multidrop Combi Reagent Dispenser (Thermo Fisher

Scientific). IC_{50} values were determined with 11- or 23-point inhibition curves in triplicate.

Structure Determination

Prior to crystallization, 0.1 mmol/L of $EGFR^{T790M/V948R}$ was purified in the presence of 2 μmol/L JBJ-04-125-02, 1 mmol/L Adenosine 5′-(β,γ-imido)triphosphate (AMP-PNP), and 10 mmol/L $MgCl_2$ by size-exclusion chromatography. Final concentration of JBJ-04-125-02 in protein solution was 20 μmol/L. Crystals of $EGFR^{T790M/V948R}$ in complex with JBJ-04-125-02 were prepared by hanging-drop vapor diffusion method over a reservoir solution containing 0.1 mol/L Bis-Tris pH 5.5, 25% PEG-3350, 5 mmol/L Tris (2-carboxyethyl)-phosphine (TCEP). Crystals were flash-frozen in liquid nitrogen after rapid immersion in a cryoprotectant solution containing 0.1 mol/L Bis-Tris 5.5, 25% PEG-3350, 20% Glycerol, and 5 mmol/L TCEP. Diffraction data was collected using a wavelength of 0.979Å on the NE-CAT beamlines ID24-C and E, Argonne National Laboratory, at 100 K. Data were processed and merged as described previously (8). The structure was determined by molecular replacement with the program PHASER using an inactive EGFR kinase structure (PDB 5D41) as the search model. Repeated rounds of manual refitting and crystallographic refinement were performed using COOT and REFMAC. The inhibitor was modeled into the closely fitting positive Fo-Fc electron density and then included in following refinement cycles. Topology and parameter files for the inhibitors were generated using PRODRG. Statistics for diffraction data processing and structure refinement are shown in Supplementary Table S1.

Cell Viability Assays

Ba/F3, H1975, H3255GR, and H3255DR cells were treated with increasing concentrations of inhibitors for 72 hours and growth or the inhibition of growth was assessed by MTS assay according to previously established methods (9, 21, 25). For experiments that investigate the effect of JBJ-04-125-02 in the presence of EGF (Life Technologies; PHG0311L) or cetuximab (Lilly; NDC 66733-948-23), 10 ng/mL of EGF, 1 μg/mL or 10 μg/mL of cetuximab was added at the same time that cells were treated with inhibitors.

Antibodies and Western Blotting

Ba/F3, NIH-3T3, H1975, H3255GR cells were treated for 4 to 24 hours before cells were lysed with NP40 lysis buffer and processed for Western blotting analyses. For experiments that examine the effect of JBJ-04-125-02 in the presence or absence of EGF, cells were treated with 10 ng/mL of EGF for 15 minutes before they were treated with drugs followed by lysis and processing as described above. The phospho-EGFR (Tyr1068; #3777, 1:1,000), EGFR (#4267; 1:2,000), phospho-AKT (Ser473; #4060, 1:2,000), AKT (#9272, 1:2,000), phospho-ERK1/2 (Thr202/Tyr204; #4370, 1:1,000), ERK1/2 (#4695, 1:2,000), and PARP (#9582, 1:1,000) antibodies were purchased from Cell Signaling Technology. Tubulin was purchased from Sigma Aldrich (T5168).

In Vivo *Studies*

All breeding, mouse husbandry, and *in vivo* experiments were performed with the approval of the Dana-Farber Cancer Institute (Boston, MA) Animal Care and Use Committee. Details of all *in vivo* studies are described in the Supplemental Methods section.

ENU Mutagenesis

ENU was purchased from Sigma Aldrich and mutagenesis studies were carried as described previously (25). Briefly, 1×10^6 cells/mL of $EGFR^{L858R}$ and $EGFR^{L858R/T790M}$ Ba/F3 cells were treated with 50 μg/mL of ENU for 24 hours before the cells were washed in RPMI media and allowed to expand. A total of 1×10^4 cells per well were plated in 96 wells, and 5 plates were plated per condition. These cells were treated continuously with DMSO, 1 μmol/L gefitinib, 1 μmol/L osimertinib, 10 μmol/L JBJ-04-125-02 alone or with gefitinib/JBJ or osimertinib/JBJ drug combinations with media and drug change once a week. Cell growth was monitored and the number of resistant colonies was counted and expanded.

IncuCyte Studies

H3255GR and H1975 cells were treated with different inhibitors and monitored by the automated microscopy using the IncuCyte Live-Cell Imaging Analysis System (Essen Bioscience). Confluency was measured by averaging the percentage of area that the cells occupied from three images of a given well every two hours for 72 hours in short-term studies or once daily for 4 weeks in long-term studies. For apoptosis studies, cells were treated with inhibitors incubated in media containing the CellEvent Caspase 3/7 Green ReadyProbes reagent (Thermo Fisher Scientific; R37111) and monitored for change in green fluorescence activity using the aforementioned imaging system. The average number of objects that were stained with green from three images per well was counted as positive for Caspase 3/7, indicating apoptosis, and recorded every two hours for 72 hours.

Statistical Analyses

The specific statistical tests used for analyzing relevant experiments are indicated in the figure legends. $P < 0.05$ was considered statistically significant.

For structural modeling of inhibitor binding, pharmacokinetic assays, *in vivo* studies, cross-linking, and biotinylated drug pull-down assays, please see Supplementary Methods.

Disclosure of Potential Conflicts of Interest

S.E. Dahlberg is a consultant/advisory board member for AstraZeneca. K.-K. Wong reports receiving commercial research support from Medimmune, Janssen, Pfizer, Takeda, Merck, and Novartis, and has ownership interest (including stock, patents, etc.) in G1 Therapeutics. M.J. Eck reports receiving a commercial research grant from Novartis Institutes for Biomedical Research, reports receiving other commercial research support from Takeda, and is a consultant/advisory board member for Novartis Institutes for Biomedical Research. N.S. Gray reports receiving a commercial research grant from Takeda and is a consultant/advisory board member for C4, Syros, Soltego, and B2S Bio. P.A. Jänne reports receiving commercial research grants from AstraZeneca, Boehringer Ingelheim, Astellas Pharmaceuticals, PUMA, Eli Lilly, and Takeda Oncology, has ownership interest (including stock, patents, etc.) in Gatekeeper Pharmaceuticals and LOXO Oncology, is a consultant/advisory board member for AstraZeneca, Boehringer Ingelheim, Daiichi Sankyo, Roche/Genentech, Pfizer, Merrimack Pharmaceuticals, Chugai Pharmaceuticals, Araxes Pharmaceuticals, Mirati, Ignyta, and LOXO Oncology, and has received other remuneration from Labcorp. No potential conflicts of interest were disclosed by the other authors.

Authors' Contributions

Conception and design: C. To, J. Jang, T. Chen, E. Park, M. Mushajiang, M.J. Eck, N.S. Gray, P.A. Jänne

Development of methodology: C. To, J. Jang, T. Chen, E. Park, M. Mushajiang, T.W. Gero

Acquisition of data (provided animals, acquired and managed patients, provided facilities, etc.): C. To, J. Jang, T. Chen, E. Park, M. Xu, S. Wang, M.D. Cameron, D.E. Heppner, A. Yang, K.-K. Wong, N.S. Gray

Analysis and interpretation of data (e.g., statistical analysis, biostatistics, computational analysis): C. To, J. Jang, T. Chen, E. Park,

M. Mushajiang, M. Xu, M.D. Cameron, A. Yang, S.E. Dahlberg, K.-K. Wong, M.J. Eck, N.S. Gray, P.A. Jänne
Writing, review, and/or revision of the manuscript: C. To, J. Jang, E. Park, D.J.H. De Clercq, M.J. Eck, N.S. Gray, P.A. Jänne
Administrative, technical, or material support (i.e., reporting or organizing data, constructing databases): C. To, M. Mushajiang, B.H. Shin
Study supervision: C. To, M.J. Eck, N.S. Gray, P.A. Jänne
Other (synthesis of some compounds used in this manuscript): D.J.H. De Clercq

Acknowledgments

This work was supported by the NCI grants R01CA135257 (to P.A. Jänne), R01CA201049 (to P.A. Jänne, M.J. Eck, and N.S. Gray), R35 CA220497 (to P.A. Jänne), and P01CA154303 (to P.A. Jänne, M.J. Eck, K.K. Wong, and N.S. Gray); The American Cancer Society (CRP-17-111-01-CDD; to P.A. Jänne); the Ildiko Medve and Adria Sai-Halasz EGFR Lung Cancer Research Fund (to P.A. Jänne); and the Balassiano Family Fund for Lung Cancer Research (to P.A. Jänne). We acknowledge support from the ICCB-Longwood Screening Facility at Harvard Medical School (to M.J. Eck).

The costs of publication of this article were defrayed in part by the payment of page charges. This article must therefore be hereby marked *advertisement* in accordance with 18 U.S.C. Section 1734 solely to indicate this fact.

Received August 10, 2018; revised March 29, 2019; accepted May 1, 2019; published first May 15, 2019.

REFERENCES

1. Paez JG, Janne PA, Lee JC, Tracy S, Greulich H, Gabriel S, et al. EGFR mutations in lung cancer: correlation with clinical response to gefitinib therapy. Science 2004;304:1497–500.
2. Lynch TJ, Bell DW, Sordella R, Gurubhagavatula S, Okimoto RA, Brannigan BW, et al. Activating mutations in the epidermal growth factor receptor underlying responsiveness of non-small-cell lung cancer to gefitinib. N Engl J Med 2004;350:2129–39.
3. Shigematsu H, Lin L, Takahashi T, Nomura M, Suzuki M, Wistuba II, et al. Clinical and biological features associated with epidermal growth factor receptor gene mutations in lung cancers. J Natl Cancer Inst 2005;97:339–46.
4. Mok TS, Wu YL, Thongprasert S, Yang CH, Chu DT, Saijo N, et al. Gefitinib or carboplatin-paclitaxel in pulmonary adenocarcinoma. N Engl J Med 2009;361:947–57.
5. Zhou C, Wu YL, Chen G, Feng J, Liu XQ, Wang C, et al. Erlotinib versus chemotherapy as first-line treatment for patients with advanced EGFR mutation-positive non-small-cell lung cancer (OPTIMAL, CTONG-0802): a multicentre, open-label, randomised, phase 3 study. Lancet Oncol 2011;12:735–42.
6. Sequist LV, Yang JC, Yamamoto N, O'Byrne K, Hirsh V, Mok T, et al. Phase III study of afatinib or cisplatin plus pemetrexed in patients with metastatic lung adenocarcinoma with EGFR mutations. J Clin Oncol 2013;31:3327–34.
7. Yu HA, Arcila ME, Rekhtman N, Sima CS, Zakowski MF, Pao W, et al. Analysis of tumor specimens at the time of acquired resistance to EGFR-TKI therapy in 155 patients with EGFR-mutant lung cancers. Clin Cancer Res 2013;19:2240–7.
8. Yun CH, Mengwasser KE, Toms AV, Woo MS, Greulich H, Wong KK, et al. The T790M mutation in EGFR kinase causes drug resistance by increasing the affinity for ATP. Proc Natl Acad Sci U S A 2008;105:2070–5.
9. Zhou W, Ercan D, Chen L, Yun CH, Li D, Capelletti M, et al. Novel mutant-selective EGFR kinase inhibitors against EGFR T790M. Nature 2009;462:1070–4.
10. Cross DA, Ashton SE, Ghiorghiu S, Eberlein C, Nebhan CA, Spitzler PJ, et al. AZD9291, an irreversible EGFR TKI, overcomes T790M-mediated resistance to EGFR inhibitors in lung cancer. Cancer Discov 2014;4:1046–61.
11. Yang JC, Ahn MJ, Kim DW, Ramalingam SS, Sequist LV, Su WC, et al. Osimertinib in pretreated T790M-positive advanced non-small-cell lung cancer: AURA study phase II extension component. J Clin Oncol 2017;35:1288–96.
12. Goss G, Tsai CM, Shepherd FA, Bazhenova L, Lee JS, Chang GC, et al. Osimertinib for pretreated EGFR Thr790Met-positive advanced non-small-cell lung cancer (AURA2): a multicentre, open-label, single-arm, phase 2 study. Lancet Oncol 2016;17:1643–52.
13. Mok TS, Wu YL, Ahn MJ, Garassino MC, Kim HR, Ramalingam SS, et al. Osimertinib or platinum-pemetrexed in EGFR T790M-positive lung cancer. N Engl J Med 2017;376:629–40.
14. Ramalingam SS, Yang JC, Lee CK, Kurata T, Kim DW, John T, et al. Osimertinib as first-line treatment of EGFR mutation-positive advanced non-small-cell lung cancer. J Clin Oncol 2017;36:841–9.
15. Soria JC, Ohe Y, Vansteenkiste J, Reungwetwattana T, Chewaskulyong B, Lee KH, et al. Osimertinib in untreated EGFR-mutated advanced non-small-cell lung cancer. N Engl J Med 2018;378:113–25.
16. Oxnard GR, Hu Y, Mileham KF, Husain H, Costa DB, Tracy P, et al. Assessment of resistance mechanisms and clinical implications in patients with EGFR T790M-positive lung cancer and acquired resistance to osimertinib. JAMA Oncol 2018;4:1527–34.
17. Thress KS, Paweletz CP, Felip E, Cho BC, Stetson D, Dougherty B, et al. Acquired EGFR C797S mutation mediates resistance to AZD9291 in non-small cell lung cancer harboring EGFR T790M. Nat Med 2015;21:560–2.
18. Jia Y, Yun CH, Park E, Ercan D, Manuia M, Juarez J, et al. Overcoming EGFR(T790M) and EGFR(C797S) resistance with mutant-selective allosteric inhibitors. Nature 2016;534:129–32.
19. Zhang X, Gureasko J, Shen K, Cole PA, Kuriyan J. An allosteric mechanism for activation of the kinase domain of epidermal growth factor receptor. Cell 2006;125:1137–49.
20. Fabian MA, Biggs WH 3rd, Treiber DK, Atteridge CE, Azimioara MD, Benedetti MG, et al. A small molecule-kinase interaction map for clinical kinase inhibitors. Nat Biotechnol 2005;23:329–36.
21. Engelman JA, Mukohara T, Zejnullahu K, Lifshits E, Borras AM, Gale CM, et al. Allelic dilution obscures detection of a biologically significant resistance mutation in EGFR-amplified lung cancer. J Clin Invest 2006;116:2695–706.
22. Pao W, Miller VA, Politi KA, Riely GJ, Somwar R, Zakowski MF, et al. Acquired resistance of lung adenocarcinomas to gefitinib or erlotinib is associated with a second mutation in the EGFR kinase domain. PLoS Med 2005;2:1–11.
23. Ercan D, Zejnullahu K, Yonesaka K, Xiao Y, Capelletti M, Rogers A, et al. Amplification of EGFR T790M causes resistance to an irreversible EGFR inhibitor. Oncogene 2010;29:2346–56.
24. Cho J, Chen L, Sangji N, Okabe T, Yonesaka K, Francis JM, et al. Cetuximab response of lung cancer-derived EGF receptor mutants is associated with asymmetric dimerization. Cancer Res 2013;73:6770–9.
25. Ercan D, Choi HG, Yun CH, Capelletti M, Xie T, Eck MJ, et al. EGFR mutations and resistance to irreversible pyrimidine-based EGFR inhibitors. Clin Cancer Res 2015;21:3913–23.
26. Wang Z, Yang JJ, Huang J, Ye JY, Zhang XC, Tu HY, et al. Lung Adenocarcinoma harboring EGFR T790M and in trans C797S responds to combination therapy of first- and third-generation EGFR TKIs and shifts allelic configuration at resistance. J Thorac Oncol 2017;12:1723–7.
27. Swain SM, Baselga J, Kim SB, Ro J, Semiglazov V, Campone M, et al. Pertuzumab, trastuzumab, and docetaxel in HER2-positive metastatic breast cancer. N Engl J Med 2015;372:724–34.
28. Robert C, Karaszewska B, Schachter J, Rutkowski P, Mackiewicz A, Stroiakovski D, et al. Improved overall survival in melanoma with combined dabrafenib and trametinib. N Engl J Med 2015;372:30–9.

29. Soh J, Okumura N, Lockwood WW, Yamamoto H, Shigematsu H, Zhang W, et al. Oncogene mutations, copy number gains and mutant allele specific imbalance (MASI) frequently occur together in tumor cells. PLoS One 2009;4:e7464.
30. Zhang J, Iwanaga K, Choi KC, Wislez M, Raso MG, Wei W, et al. Intratumoral epiregulin is a marker of advanced disease in non-small cell lung cancer patients and confers invasive properties on EGFR-mutant cells. Cancer Prev Res 2008;1:201–7.
31. Wylie AA, Schoepfer J, Jahnke W, Cowan-Jacob SW, Loo A, Furet P, et al. The allosteric inhibitor ABL001 enables dual targeting of BCR-ABL1. Nature 2017;543:733–7.
32. Zhang J, Adrian FJ, Jahnke W, Cowan-Jacob SW, Li AG, Iacob RE, et al. Targeting Bcr-Abl by combining allosteric with ATP-binding-site inhibitors. Nature 2010;463:501–6.
33. Yun CH, Boggon TJ, Li Y, Woo MS, Greulich H, Meyerson M, et al. Structures of lung cancer-derived EGFR mutants and inhibitor complexes: mechanism of activation and insights into differential inhibitor sensitivity. Cancer Cell 2007;11:217–27.
34. Hong L, Quinn CM, Jia Y. Evaluating the utility of the HTRF Transcreener ADP assay technology: a comparison with the standard HTRF assay technology. Anal Biochem 2009;391:31–8.